Current Science
CS 5 (4), 4286-4294 (2025)
Received 25 May 2025 | **Revised 25 June** 2025 | **Accepted 26 July**. 2025 | **Online Available 31 August** 2025
https://doi.org/10.52845/CS/2025-5-4-74

Current Science
Current Science

OPEN ACCESS

ISSN(O)2795-8639

Original Article

Comparative Analysis of Gut Microbial Diversity and Composition Changes after CMPI Treatment in CINP Model

Fengchai Wang[1], Yujia Luo[2*]

[1]Putian First Hospital, Putian, China

[2]The First Affiliated Hospital, Zhejiang University School of Medicine, Hangzhou, China

[*]Corresponding Author: Yujia Luo

Abstract:
Chemotherapy-induced neuropathic pain (CINP) significantly affects the quality of life for cancer survivors, with limited effective treatment options currently available. The α4β2 nicotinic acetylcholine receptor (nAChR) has emerged as a potential target for CINP treatment. This study investigates the impact of an α4β2 nAChR positive allosteric modulators on gut microbiota. Wild-type C57BL/6 mice were used to establish a CINP model through oxaliplatin administration. Gut microbiota composition was analyzed using 16S rRNA gene sequencing, followed by bioinformatics methods to assess microbial diversity and community structure. High-throughput sequencing revealed notable alterations in gut microbial diversity and composition post-CMPI treatment, including decreased Desulfobacterota and increased Clostridia abundance, which may be linked to the drug's analgesic and anti-inflammatory effects. CMPI is potentially acting through modulation of the gut microbiota. Further research is needed to clarify the mechanisms and their implications for pain relief.

Keywords: Chemotherapy-induced neuropathic pain; α4β2 nicotinic acetylcholine receptor; CMPI; Gut microbiota; allosteric modulator.

1 Introduction

Chemotherapy-induced neuropathic pain (CINP) is a complex and debilitating condition that often results in chronic discomfort and distress for cancer survivors[1]. It is one of the most difficult chronic pains to treat clinically[1,2]. Statistics show that about 70% of cancer patients will experience CINP after multiple chemotherapy sessions, which severely limits the application and dosage adjustment of chemotherapy drugs and imposes a significant burden on the lives and economy of cancer chemotherapy patients[3-5]. Currently, there are no effective treatment options with minimal side effects available in the clinic[6]. The commonly used treatments include first-line antidepressants and anticonvulsants acting on calcium channels, and second- and third-line local lidocaine and opioid drugs, which often have poor efficacy, are only effective for a small number of patients, and come with side effects[7]. Therefore, there is an urgent need to explore new targets for the treatment of CINP.

The α4β2 nicotinic acetylcholine receptor (nAChR), a key receptor subtype in the central and peripheral nervous systems, has been identified as a significant player in pain modulation[8-10]. Given its strategic role in neurotransmission, particularly in brain regions involved in pain processing, the α4β2 nAChR presents a promising target for therapeutic intervention in neuropathic pain[9,11-14]. However, the potential influence of high-selectivity α4β2 nAChR positive allosteric modulators (e.g. CMPI) on the gut microbiota and its implications for the 'brain-gut axis' have not been thoroughly investigated. This study aims to fill this gap by examining the effects of CMPI on gut microbial

diversity and composition in a CINP model using 16S rRNA gene sequencing.

Our research focuses on the modulation of the gut microbiota by CMPI. By comparing the gut microbiota profiles of CINP model mice with those treated with CMPI, we aim to identify specific microbial changes associated with the therapeutic effects of the drug.

Methods

Experimental Animal

Wild-type C57BL/6 mice were sourced from the Zhejiang Academy of Medical Sciences (SCXK (Zhejiang) 2024-0037) and bred at the Laboratory Animal Department of Zhejiang University. The Laboratory Animal Department of Zhejiang University can provide barrier facilities for germ-free breeding.

CINP Model

The CINP model in C57BL/6 mice was established according to the oxaliplatin dosage recommended by the World Health Organization (administering 2-3 mg/kg oxaliplatin twice a week for a total of 9 injections). The up-and-down method using von-Frey filaments (0.02, 0.04, 0.07, 0.16, 0.4, 0.6, 1, 2g) was applied, along with observations of whether the mice exhibited reduced food intake, weight loss, and slowed weight gain, to determine the success of the model construction.

Data Processing

Sample data were demultiplexed based on barcode and primer sequences[15]. FLASH (Version 1.2.11) was used to merge paired-end reads, generating raw tags. High-quality tags were obtained through stringent filtering using fastp software (Version 0.23.1). Chimera sequences were identified and removed by aligning tags against species annotation databases (Silva database for 16S/18S, Unite database for ITS), resulting in effective tags[16,17]. Effective Tags were denoised using the DADA2 module or deblur in QIIME2 (Version QIIME2-202202), yielding amplicon sequence variants (ASVs) and a feature table. Species annotation was conducted using QIIME2 software with the Silva 138.1 database for 16S and 18S, and the Unite v8.2 database for ITS. A rapid multiple sequence alignment was performed using QIIME2 software to determine the phylogenetic relationships among all ASV sequences. Data from each sample were normalized based on the sample with the least amount of data, and subsequent alpha and beta diversity analyses were conducted using normalized data. The top 10 species at different taxonomic ranks (class, order, family, genus, species) in each sample were visualized using SVG functions to create histograms of relative abundance. A phylogenetic tree, also known as an evolutionary tree, was constructed to describe the evolutionary relationships among different species. The 100 most abundant genera were selected for sequence alignment, and an SVG-formatted phylogenetic tree was plotted using Perl.

Statistical Analyses

A series of statistical analyses, including Anosim, Adonis, MRPP, Simper, T-tests, MetaStat, and LEfSe, were employed to reveal the differentiation of community structures. QIIME2 software was utilized to calculate observed_otus, shannon, simpson, chao1, goods_coverage, dominance, and pielou_e indices. Detailed descriptions of these indices are provided in the references. Beta diversity analysis was conducted in QIIME2 based on weighted and unweighted distances to assess the complexity of community composition and differences between groups. A UPGMA (Unweighted Pair Group Method with Arithmetic Mean) clustering tree was constructed based on the weighted unifrac distance matrix. This method is widely used in ecology for evolutionary classification. UPGMA plots were generated using the UPGMA.tre function in Qiime. Principal Component Analysis (PCA), PCoA (Principal Coordinates Analysis), and NMDS (Non-Metric Multidimensional Scaling) were used to reduce the dimensionality of complex and multidimensional data. PICRUSt (V1.1.4) and its improved version, PICRUSt2 (V2.3.0), were used to predict metagenome functions based on marker genes. Tax4Fun (V0.3.1), BugBase, and FunGuild tools were utilized for functional predictions and analysis of microbial communities. Two-dimensional and three-dimensional network graphs were constructed to explore symbiotic relationships between species and the impact of environmental factors on community structure. Correlation analyses, CCA/RDA, and dbRDA were used to further investigate the correlation between environmental factors and species abundance. All

analyses and visualizations were completed using R. Throughout the analysis, Python, R, and Perl versions 3.6.13, 4.0.3, and 5.26.2 were utilized, respectively.

Results

Species Visualization of Gut Microbiota

In this study, high-throughput sequencing of the V3-V4 regions of the 16S rDNA of gut microbiota from C57BL/6J in the CINP group and CMPI group was conducted. The raw data of each sample were obtained according to the barcode, and the barcode and primers were removed. The R1 and R2 sequence data were then assembled using the FLASH software. After quality control of the assembled tags, clean tags were obtained, and chimera filtering was performed to yield 716,043 effective sequences available for subsequent analysis.

The DADA2 method was selected for data processing, which differs from the traditional Operational Taxonomic Units (OTU) clustering method by only performing deduplication. Each deduplicated sequence produced by DADA2 noise reduction is referred to as ASVs (Amplicon Sequence Variants), or feature sequences (corresponding to the representative sequences of OTU in similarity clustering methods). The DADA2 method is more sensitive and specific than the traditional OTU method, capable of detecting real biological variations omitted by the OTU method while outputting fewer false sequences.

Additionally, the replacement of OTUs with ASVs improves the accuracy, comprehensiveness, and reproducibility of marker gene data analysis. The QIIME2 classify-sklearn algorithm was used to annotate each ASV using a pre-trained Naive Bayes classifier. Based on the ASVs annotation results and the feature table of each sample, species abundance tables at the levels of Kingdom, Phylum, Class, Order, Family, Genus, and Species were obtained. These annotated abundance tables are the core content of amplicon analysis.

Depending on the experimental purpose, one or several key species can be selected from the species abundance tables at various taxonomic levels (usually focusing on the Phylum and Genus levels), and in-depth studies can be conducted in combination with the species composition and difference analysis, clustering analysis, and other results of different groups. The species box plot shows an increase in the number of observed species with the increase in sample size. When the number of samples is between 0 and 30, the number of species increases significantly with the increase in sample size. When the sample size reaches 30, the increase in the number of observed species is not significant, and the curve gradually becomes flat. The results indicate that the species observed in the samples are gradually stabilizing and will not significantly increase due to the increase in sample size. This suggests that the fecal sample size collected in this study is sufficient and adequately sampled for high-throughput sequencing data analysis.

Species Abundance of Gut Microbiota

Based on the species annotation results at different taxonomic levels, the top 10 species with the highest relative abundance for each sample or group at the levels of Phylum, Class, Order, Family, Genus, and Species were selected, and the remaining species were set as Others. Bar charts of the species annotation results at different taxonomic levels corresponding to each sample were drawn (**Figure 1A**).

At the Phylum level, the top ten bacterial phyla in the gut microbiota of SPF-grade CINP group mice and CMPI-treated mice mainly include Bacteroidetes (average proportion of 45.4%), Firmicutes (37.9%), Desulfobacterota (4.8%), Actinobacteriota (3.5%), Verrucomicrobiota, Proteobacteria, Actinobacteria, Campylobacterota, Cyanobacteria, Fusobacteriota, Myxococcota, and Crenarchaeota, accounting for about 99% of the total sequence number. The remaining phyla account for less than 1% of the total number, with Bacteroidetes and Firmicutes accounting for about 83% of the total, being the dominant bacteria in the gut microbiota. Among them, the proportion of Desulfobacterota in the CINP group (9.1%) is significantly higher than that in the CMPI treatment group (0.4%). These bacteria are anaerobic bacteria that mainly use sulfate as an electron acceptor for sulfur reduction reactions, producing hydrogen sulfide. At the Class level, the top ten bacterial classes in the gut microbiota of CINP modeling mice and CMPI-treated mice mainly include Bacteroidia (average proportion of 45.4%), Bacilli (21.8%), Clostridia (16.0%), Saccharimonadia (4.4%), Desulfovibrionia,

Coriobacteriia, Verrucomicrobiae, Gammaprote obacteria, unidentified_Actinobacteria, accounting for about 98.7% of the total. The remaining 99 classes account for less than 5% of the total, with Bacteroidia, Clostridia, and Bacilli accounting for more than 83% of the total, being the dominant bacteria in the gut microbiota. Among them, the proportion of Clostridia in the CINP group (0.9%) is significantly lower than that in the CMPI treatment group (2.1%) ($P < 0.05$). Clostridia is a class of Gram-positive bacteria belonging to the Firmicutes phylum. Some bacteria in this class, such as Clostridium butyricum, can produce butyric acid and other short-chain fatty acids, which help maintain the health of the intestinal mucosa (**Figure 1B**).

To further study the systematic evolutionary relationships of species at the genus level, multiple sequence alignments were performed to obtain representative sequences of the top 100 genera and are shown in **Figure 1C**.

Based on the species annotation and abundance information at the genus level for all samples, the top 35 genera with the highest abundance were selected. The abundance information of these genera in each sample was used to cluster from the species level and draw a heat map, facilitating the discovery of the high and low content of species aggregation in the CMPI group and control group (**Figure 1D**).

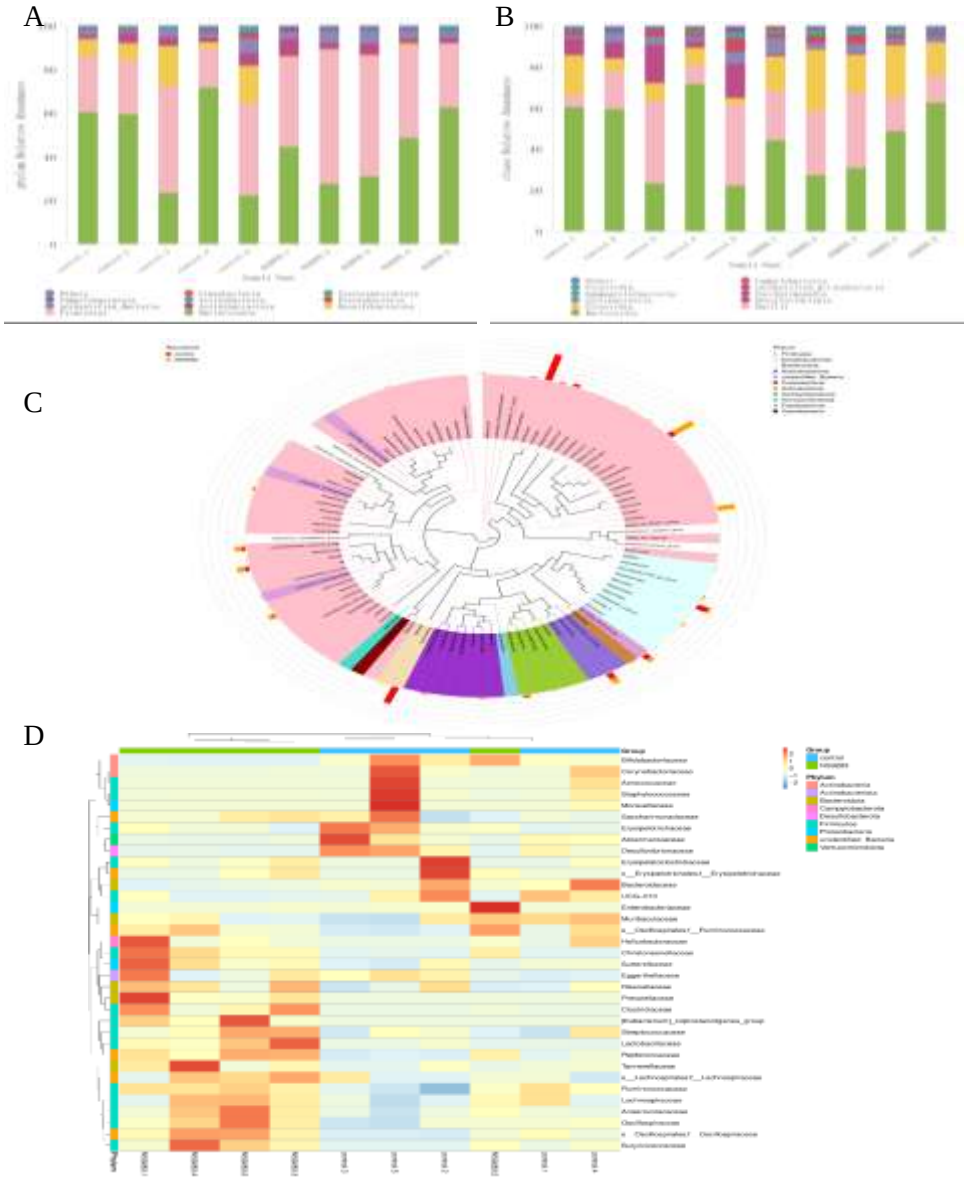

Figure 1. Bar chart of species relative abundance at the (A) Phylum level and (B) Class level. (C) Representative sequences of the top 100 genera. (D) Heat map facilitating the discovery of the high and low content of species aggregation.

Species Diversity of Gut Microbiota

The dilution curve is a common curve used to describe the diversity within a group of samples. It is constructed by randomly extracting a certain amount of sequencing data from the samples and analyze their alpha diversity index values, using the amount of sequencing data extracted and the corresponding index values to build the curve. When the curve becomes flat, it indicates that the amount of sequencing data is reasonable, and more sequencing data will only produce a small number of new OTUs. The results show that as the amount of sequencing increases, the dilution curves for each sample gradually become flat. Most samples show an inflection point when the sequencing amount reaches about 2000, indicating that the amount of OTUs does not increase significantly when the sequencing amount exceeds 2000; when the sample sequencing amount reaches 30,000, the dilution curve becomes essentially flat, indicating that the amount of OTUs no longer increases significantly when the sequencing amount exceeds 30,000. In this study, the average sequencing amount for all samples is 37,771, indicating that the sequencing depth and coverage are sufficient, and the species are rich. The samples are suitable for further analysis and research. The relationship curve between the chao1 index and the sequencing amount for each sample is shown in **Figure 2**.

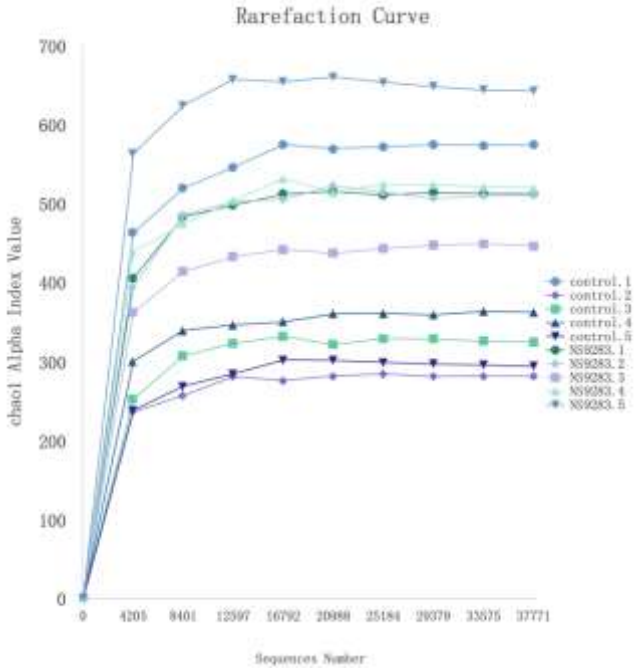

Figure 2. The relationship curve between the chao1 index and the sequencing amount for each sample. The horizontal axis represents the amount of sequencing data, and the vertical axis represents the corresponding alpha diversity index. When the curve becomes flat, it indicates that the amount of sequencing data is gradually reasonable, and more data will not significantly affect the alpha diversity index.

α-Diversity can be used to reflect the richness and diversity of the microbial community within a single sample, including shannon, simpson, Chao1, ACE, Good's coverage, and index analysis. The α-diversity index differences between the control group and the CMPI treatment group are shown in **Figure 3A**, where the chao1 index and observed index, which reflect richness, are lower in the control group than in the CMPI treatment group ($P > 0.05$).

Non-Metric Multi-Dimensional Scaling is a ranking method suitable for ecological research. NMDS is a nonlinear model based on Weighted_unifrac and Unweighted_unifrac distances for analysis. It reflects the species information contained in the samples in the form of points on a two-dimensional plane. Its design purpose is to overcome the shortcomings of linear models (including PCA, PCoA) and better reflect the nonlinear structure of ecological data. Applying NMDS analysis, the species information

contained in the samples is reflected in the form of points on a multidimensional space, and the degree of difference between different samples is reflected through the distance between points (**Figure 3B**).

Principal Component Analysis is a method based on Euclidean distances for variance decomposition. It reduces high-dimensional data through dimensionality reduction to extract the most significant elements and structures in the data. Applying PCA analysis enables the extraction of the two coordinate axes that most significantly reflect the differences between samples, thereby reflecting the differences in multidimensional data on a two-dimensional coordinate graph and revealing simple patterns in the background of complex data. If the community composition of the samples is similar, they will be closer in the PCA graph. The PCA analysis results based on feature sequence levels are shown in **Figure 3C**.

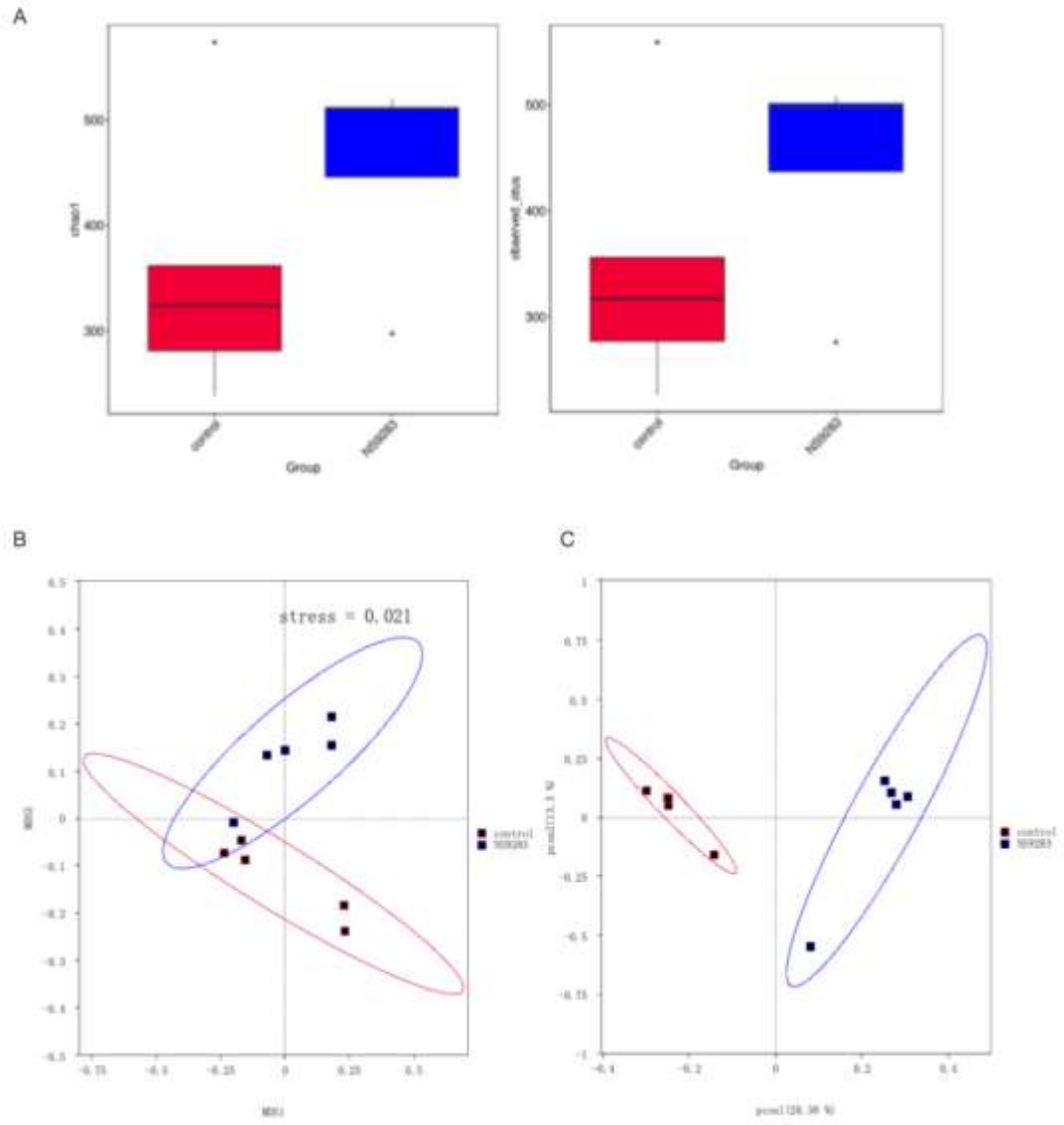

Figure 3. (A) The α-diversity index differences between the control group and the CMPI treatment group. (B) The α-diversity index differences between the control group and the CMPI treatment group. Each point in the figure represents a sample, and the distance between points indicates the degree of difference. Samples from the same group are represented in the same color. A Stress value less than 0.2 indicates that NMDS can accurately reflect the degree of difference between samples. The species information contained in the samples is reflected in the form of points on a multidimensional space, and the degree of difference between different samples is reflected through the distance between points. (C) The PCA analysis results based on feature sequence levels.

Discussion

The present study has undertaken a comprehensive examination of the gut microbiota in CINP model mice and those treated with CMPI. Utilizing 16S rRNA gene sequencing, we have identified significant alterations in the gut microbial diversity and composition that are associated with CMPI treatment. These findings provide valuable insights into the potential role of the gut microbiota in the analgesic effects of CMPI and contribute to the broader understanding of the 'brain-gut axis' in pain modulation.

One of the key observations from our results is the notable decrease in the relative abundance of Desulfobacterota in the CMPI-treated group compared to the CINP model mice. This bacterial group is known to be involved in sulfate reduction and has been linked to intestinal inflammation. The reduction of Desulfobacterota with CMPI treatment may suggest a mechanism by which the drug could be reducing inflammation and potentially contributing to its analgesic effects[18]. This observation warrants further investigation into the specific role of Desulfobacterota in pain processing and the impact of CMPI on this bacterial group. Additionally, our results indicate an increase in the Clostridia class in the gut microbiota of mice treated with CMPI. Clostridia, particularly those that produce short-chain fatty acids like butyrate, are recognized for their beneficial effects on gut health, including anti-inflammatory properties. The increase in Clostridia may indicate a positive shift in the gut microbiota that could be associated with the analgesic effects of CMPI. This finding aligns with the growing body of evidence that supports the role of gut health in systemic inflammation and pain modulation[19].

The use of advanced bioinformatics tools and high-throughput sequencing in our study has allowed for a detailed characterization of the gut microbial community. The identification of these specific changes in microbial composition provides a foundation for future research to explore the mechanistic links between gut microbiota and pain perception. However, the precise mechanisms by which CMPI influences the gut microbiota and alleviates pain remain to be elucidated. Further studies should aim to delineate the causal relationships between these microbial changes and the analgesic effects of CMPI, as well as investigate the long-term impact of such modulation on gut health and pain outcomes.

Conclusion

16S rRNA high-throughput sequencing revealed that CMPI profoundly reshapes the gut microbiota of oxaliplatin-induced CINP mice. CMPI administration led to a marked reduction in Desulfobacterota, a sulfate-reducing phylum linked to intestinal inflammation and peripheral sensitization, and a significant enrichment of the butyrate-producing Clostridia class within the Firmicutes phylum, consistent with an anti-inflammatory and gut-barrier-protective signature. An overall increase in α-diversity indices (Chao1 and observed species) and a distinct β-diversity separation (NMDS, PCA) that distinguished CMPI-treated from untreated CINP mice.

Authors Contribution: YJ.L (Conceptualization; Conceptualization; Writing-Original; Methodology; Formal Analysis; Investigation); YJ.L (Conceptualization; Writing-Review & Editing; Supervision; Project administration).

Funding: Supported by the Medicine and Health Science and Technology Project of Zhejiang Province of China (Grant No. 2024KY995).

Institutional Review Board Statement: Not applicable.

Informed Consent Statement: Not applicable.

Data Availability Statement: The datasets generated and/or analyzed during the current study are available from the corresponding author upon reasonable request.

Conflicts of Interest: The authors declare no conflict of interest.

References

1. Colvin LA. Chemotherapy-induced peripheral neuropathy: where are we now? *Pain* 2019; 160 Suppl 1(Suppl 1): S1-s10.
2. Sałat K. Chemotherapy-induced peripheral neuropathy: part 1-current state of knowledge and perspectives for pharmacotherapy. *Pharmacol Rep* 2020; 72(3): 486-507.
3. Argyriou AA, Bruna J, Kalofonou F, et al. Incidence and risk factors for developing chemotherapy-induced neuropathic pain in 500 cancer patients: A file-based observational study. *J Peripher Nerv Syst* 2024; 29(1): 38-46.

4. Antoniou G, Lambourg E, Steele JD, Colvin L A. The effect of adverse childhood experience s on chronic pain and major depression in adul thood: a systematic review and meta-analysis. *Br J Anaesth* 2023; 130(6): 729-46.
5. Scholz J, Finnerup NB, Attal N, et al. The IAS P classification of chronic pain for ICD-11: ch ronic neuropathic pain. *Pain* 2019; 160(1): 53-9.
6. Finnerup NB, Attal N, Haroutounian S, et al. P harmacotherapy for neuropathic pain in adults: a systematic review and meta-analysis. *Lancet Neurol* 2015; 14(2): 162-73.
7. Zafari N, Velayati M, Maftooh M, et al. Mech anism-based Pharmacological Management of Chemotherapy-induced Neuropathic Pain fro m Preclinical Studies to Clinical Prospective: Platinum-based Drugs, Taxanes, and Vinca Al kaloids. *Curr Pharm Des* 2023; 29(16): 1245-65.
8. Grupe M, Grunnet M, Bastlund JF, Jensen AA. Targeting α4β2 nicotinic acetylcholine recepto rs in central nervous system disorders: perspec tives on positive allosteric modulation as a the rapeutic approach. *Basic Clin Pharmacol Toxi col* 2015; 116(3): 187-200.
9. Nirogi R, Goura V, Abraham R, Jayarajan P. α 4β2* neuronal nicotinic receptor ligands (agon ist, partial agonist and positive allosteric modu lators) as therapeutic prospects for pain. *Eur J Pharmacol* 2013; 712(1-3): 22-9.
10. Wilkerson JL, Deba F, Crowley ML, Hamoud a AK, McMahon LR. Advances in the In vitro and In vivo pharmacology of Alpha4beta2 nic otinic receptor positive allosteric modulators. *Neuropharmacology* 2020; 168: 108008.
11. Bagdas D, Ergun D, Jackson A, Toma W, Schu lte MK, Damaj MI. Allosteric modulation of α 4β2* nicotinic acetylcholine receptors: Desfor mylflustrabromine potentiates antiallodynic re sponse of nicotine in a mouse model of neurop athic pain. *Eur J Pain* 2018; 22(1): 84-93.
12. Kiguchi N, Kobayashi D, Saika F, Matsuzaki S, Kishioka S. Inhibition of peripheral macrop hages by nicotinic acetylcholine receptor agon ists suppresses spinal microglial activation and neuropathic pain in mice with peripheral nerve injury. *J Neuroinflammation* 2018; 15(1): 96.
13. Li W, Cai J, Wang BH, Huang L, Fan J, Wang Y. Antinociceptive effects of novel epibatidine analogs through activation of α4β2 nicotinic re ceptors. *Sci China Life Sci* 2018; 61(6): 688-95.
14. Saika F, Kiguchi N, Kobayashi Y, Kishioka S. Peripheral alpha4beta2 nicotinic acetylcholine receptor signalling attenuates tactile allodynia and thermal hyperalgesia after nerve injury in mice. *Acta Physiol (Oxf)* 2015; 213(2): 462-71.
15. Bokulich NA, Subramanian S, Faith JJ, et al. Quality-filtering vastly improves diversity esti mates from Illumina amplicon sequencing. *Na t Methods* 2013; 10(1): 57-9.
16. Edgar RC, Haas BJ, Clemente JC, Quince C, Knight R. UCHIME improves sensitivity and speed of chimera detection. *Bioinformatics* 20 11; 27(16): 2194-200.
17. Magoč T, Salzberg SL. FLASH: fast length ad justment of short reads to improve genome ass emblies. *Bioinformatics* 2011; 27(21): 2957-63.
18. Zhang S, Li B, Zeng L, et al. Exploring the im mune-inflammatory mechanism of Maxing Sh igan Decoction in treating influenza virus A-in duced pneumonia based on an integrated strate gy of single-cell transcriptomics and systems b iology. *Eur J Med Res* 2024; 29(1): 234.
19. Liu ZZ, Zhou CK, Lin XQ, et al. STING-depe ndent trained immunity contributes to host def ense against Clostridium perfringens infection via mTOR signaling. *Vet Res* 2024; 55(1): 52.